THE JOURNAL OF PHYSICAL CHEMISTRY A
A JOURNAL OF THE AMERICAN CHEMICAL SOCIETY

pubs.acs.org/JPCA Article

Red-Shifting the Excitation Energy of Carbonic Acid Clusters Via Nonminimum Structures

Published as part of The Journal of Physical Chemistry virtual special issue "MQM 2022: The 10th Triennial Conference on Molecular Quantum Mechanics".

Olivia G. Haney, Brent R. Westbrook, Taylor J. Santaloci, and Ryan C. Fortenberry*

Cite This: https://doi.org/10.1021/acs.jpca.2c07589 Read Online

ACCESS | Metrics & More | Article Recommendations | Supporting Information

ABSTRACT: Nonminimum carbonic acid clusters provide excitation energies and oscillator strengths in line with observed ice-phase UV absorptions better than traditional optimized minima. This equation-of-motion coupled cluster quantum chemical analysis on carbonic acid monomers and dimers shows that shifts to the dihedral angle for the internal heavy atoms in the monomer produce UV electronic excitations close to 200 nm with oscillator strengths that would produce observable features. This τ(OCOO) dihedral is actually a relatively floppy motion unlike what is often expected for sp^2 carbons and can be distorted by 30° away from equilibrium for an energy cost of only 11 kcal/mol. As this dihedral decreases, the excitation energies decrease, as do the oscillator strengths but only to a point. Hence, the lower-energy distortions of τ(OCOO) are sufficient to produce structures that exhibit excitation energies and oscillator strengths that would red-shift observed spectra of carbonic acid ices away from the highest UV absorption feature at 139 nm. Such data imply that colder temperatures (20 K) in the experimental treatment of carbonic acid ices are freezing these structures out after annealing, whereas the warmer temperature experiments (80 K) are not.

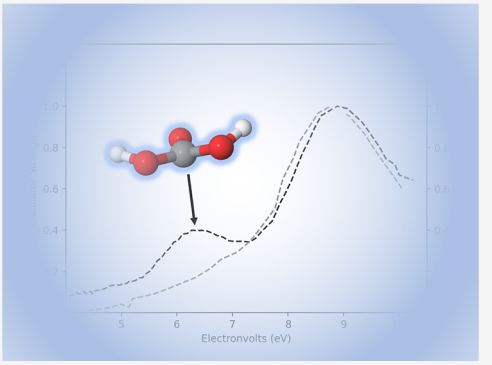

INTRODUCTION

The four central bonds of carbon are easily satiated by bonds with oxygen in the form of aldehydes and alcohols. However, while both formaldehyde and formic acid are exceptionally stable molecules and building blocks of organic chemistry, the diol form (carbonic acid, CO_3H_2), is notoriously unstable and has required modern analysis for characterization.[1,2] Case in point, the proper phase of the solid form of carbonic acid has only recently been clearly established.[3,4] Hence, the seemingly straightforward form of carbonic acid that fulfills all of the expectations for p-block and organic chemistry has remained either elusive or unclear, even recently. A similar and simpler diol, methanediol, has only been clearly observed within the past year in the gas phase, enhanced by theoretical confirmation.[5−7] As such and besides a few successes, the modern experimental production of carbonic acid under physical conditions similar to those found in nature has been stymied by its high reactivity and proclivity to remain as its painfully stable substituents: water and CO_2.

In ice experiments similar to those utilized to produce methanediol,[5] amorphous ice-phase techniques[8] have been able to produce a UV spectrum for solid carbonic acid in what is believed to be an almost exclusively amorphous phase.[9] While the motivation for such an experiment ostensibly is to produce ices that reflect astrophysical conditions, such as the outer solar system or the interstellar medium, characterization of such ice under simulated conditions should be readily handled by UV analysis. Unfortunately, the UV spectrum for the amorphous carbonic acid ice differs somewhat between two experimental approaches employed.[9] Deposition of CO_2/H_2O ices at 20 K, annealed to either 200 or 225 K and then returned to 20 K, produces a clear peak at 139 nm. This feature is attributable to an $n \rightarrow \pi^*$ excitation present in all of the examined forms of carbonic acid. This includes isolated molecules, a ribbon cluster arrangement in line with the β solid polymorph, and the amorphous phase.[9,10] However, the second experimental approach[9] deposits CO_2/H_2O ices at 80 K, anneals the ice to either 200 or 225 K, and returns it to 80 K. This approach produces the 139 nm peak, but it also exhibits a second feature at 200 nm. While this second peak is known to correspond to carbonic acid,[11] the exact molecular form or clustering arrangement of what causes this carbonic acid peak remains unknown.

Received: October 28, 2022
Revised: December 14, 2022

Previous theoretical work[10,12] indicates that the second peak likely correlates to a nonminimum orientation of carbonic acid units relative to one another. This excitation corresponds to an $n \rightarrow \sigma^*$ excitation that produces a zero oscillator strength by symmetry for the C_{2v} and C_{2h} symmetries of the isolated carbonic acid molecules and the ribbon isomers. Hence, excitations in the 200 nm range are present for all forms of carbonic acid, but the oscillator strength and intensities in turn are necessarily zero by symmetry. While these computations also indicate that all forms of carbonic acid exhibit features that produce transitions in the 139 nm range, for the 200 nm features to be observed, the symmetry likely must be broken.

Even though a previously unknown helical arrangement of carbonic acid clusters provides some red-shifted excitation energies, they still fall short of the 200 nm range[10] defined here to be from 5.5 to 7.0 eV. Furthermore, a new protocol has been developed in order to assess the electronic spectra of truly amorphous clusters producing strong correlation with benchmark experiments for amorphous solid water, ammonia, and CO_2.[13] However, treatment of amorphous carbonic acid utilizing this approach only produces the strong feature in the region of 139 nm (8.92 eV) with no notable features predicted in the range of 200 nm (again, 5.5−7.0 eV).[12] The amorphous and helical clusters actually exhibit nonzero oscillator strengths for some transitions between 5.5 and 7.0 eV wavelengths, but the oscillator strengths are typically 3 orders of magnitude or more smaller than those for the 139 nm range excitations.

On the other hand, a nonminimum, perpendicular arrangement of carbonic acid dimers in a tetramer cluster has recently been shown to exhibit $n \rightarrow \sigma^*$ excitations in the 5.5 to 7.0 eV range with oscillator strengths that are on the order of 20% the value of those for the $n \rightarrow \pi^*$ excitations closer to 8.9 eV.[10] As such, the original, higher-temperature experiments in ref 9 may be freezing out these nonminimum structures that allow for the longer-wavelength oscillator strengths to grow to observable values.

Granted, a single computation of a single arrangement in a single cluster is hardly grounds for confirmation. Hence, more characterization of how these lower-energy $n \rightarrow \sigma^*$ electronic excitations behave in carbonic acid is needed. Is the symmetry breaking attainable in moving the hydrogen atoms, or is the growth in the oscillator strength maximized by the placement of molecules in a cluster? Is it a combination of both? The present work is an attempt to address these questions in order to provide deeper insights into the nature of carbonic acid. These fundamental explorations of symmetry breaking in carbonic acid monomers and dimers will generate a more firm understanding of how carbonic acid clusters behave in the UV and likely how such inferences can be extrapolated to related systems. The goal is to inform laboratory study and astrophysical implications of prebiotic ices.

COMPUTATIONAL METHODS

The nonminimum structures are explored via scans of various dihedral angles. In order to begin, the base monomer and dimer geometries are taken from ref 10. For those structures that require new optimizations (such as nonminimum dimers), second-order Møller−Plesset perturbation theory (MP2) with the aug-cc-pVDZ basis set is used.[14−16] Once the reference geometry is selected, the dihedral angles (θ) as defined for each explored system are displaced by 3.0°, creating constrained scans. From each of these θ displacments, equation-of-motion coupled cluster theory at the singles and doubles levels (EOM-CCSD) with an aug-cc-pVTZ basis set is used to compute the vertical electronically excited states with transition energies of less than 8.0 eV.[17−19] Recent work has also shown that the reference geometry has little effect on the excitation energy, implying that the starting geometry will have no qualitative and meaningful quantitative effects on the implications of this work.[20] All quantum-chemical computations made use of the MOLPRO 2020.1 program.[21,22]

The UV spectral features in question can be modeled only as convolved spectra since several computed excitations add together to create the experimentally correlative features.[10,12] The spectra for each displacement of each scan are broadened with a 0.2 eV full width at half-maximum with Gaussian functions. These are then stacked together and given a rainbow color code across the scan in order to show how the spectra change as a function of θ.

RESULTS AND DISCUSSION

Hydrogen Atom Displacements in the Monomers. Figure 1 reports the excitation energies and oscillator strengths

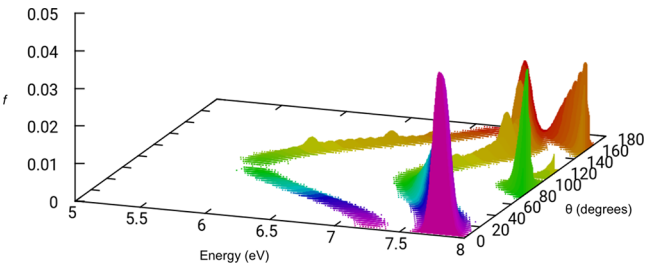

Figure 1. Conrotatory (C_2) scan of the hydrogen atoms in the carbonic acid monomer. The states reported (from left to right) are 2^1A, 1^1B, and 2^1B.

(f) for the conrotatory scan of the hydrogen atom dihedral pair in the carbonic acid monomer over θ values from 0° to 180°. This scan is represented in Figure 2A and effectively analyzes the C_2 structures between the *syn*−*syn* and the 0.49 eV higher-energy[10] *anti*−*anti* C_{2v} minima. At first glance, the lowest-energy excited state (2^1A) drops down into the spectral range desired to help explain the spectrum observed in ref 9. This $n \rightarrow \pi^*$ excitation has a zero oscillator strength by symmetry at

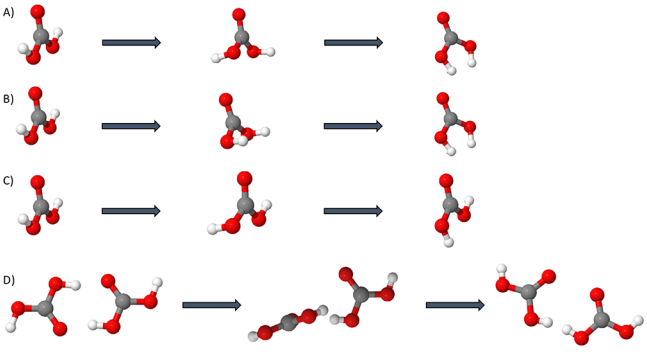

Figure 2. Visual depictions for the (A) conrotatory (C_2) scan of the hydrogen atoms in the carbonic acid monomer, (B) disrotatory (C_s) scan of the hydrogen atoms in the carbonic acid monomer, (C) single hydrogen (C_1) scan of a single hydrogen in the carbonic acid monomer, and (D) scan (C_2) of the carbonic acid dimer.

https://doi.org/10.1021/acs.jpca.2c07589
J. Phys. Chem. A XXXX, XXX, XXX−XXX

either of the C_{2v} minima, where it would be an $^1A_2$ state. While breaking the symmetry produces a nonzero excitation, the oscillator strength never strays above 0.001 for all θ values. The numerical values for the excitation energies and oscillator strengths for each displacement θ are given in the Supporting Information. As a result, this excitation, while in the 5.5−7.0 eV range as required of the 200 nm feature from ref 9, will still have little-to-no contribution due to the smaller f value. The 1^1B ($n \rightarrow \sigma^*$) state higher in energy matches the symmetry of the state observed in the perpendicular tetramer of ref 12 in the sub-7.0 eV range. Unfortunately, this excited state never drops below 7.0 eV in the scan, and the oscillator strength reduces as the excitation moves away from equilibrium.

The disrotatory scan of the hydrogen out-of-plane torsions through C_s geometries in Figure 3 actually behaves in a similar

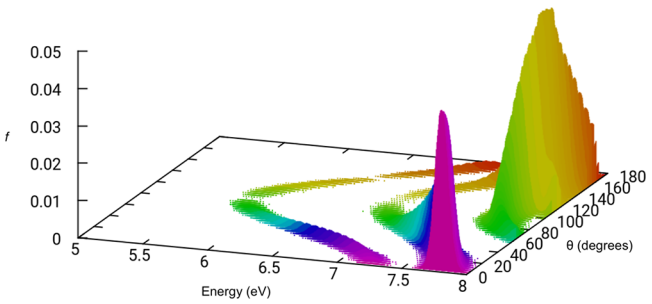

Figure 3. Disrotatory (C_s) scan from Figure 2B of the hydrogen atoms in the carbonic acid monomer. The states reported (from left to right) are $1^1A''$, $2^1A'$, and $2^1A''$.

fashion. An excited ($1^1A''$) state appears in the proper energy range, but the oscillator strength remains small across the scan and even goes to zero for the minimum excitation energy at θ = 90°. The next excited state, $2^1A'$, behaves like the 1^1B of the conrotatory scan in that its energy never drops below 7.0 eV, but the oscillator strength in this form vanishes at the minimum energy. Hence, this structure is not promising for the correlation to the experimental UV spectrum observed.

Finally for the monomers, a C_1 scan of just a single out-of-plane hydrogen torsional twist is also considered in Figure 4.

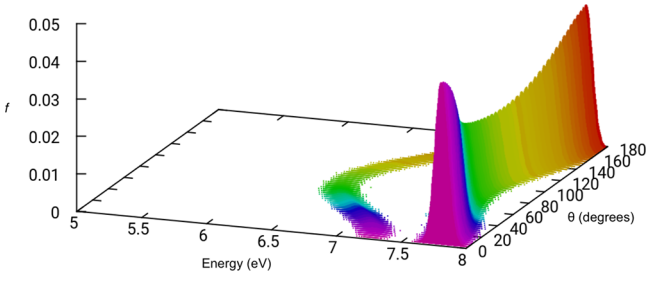

Figure 4. Single hydrogen (C_1) scan of a single hydrogen (Figure 2C) in the carbonic acid monomer. The states reported (from left to right) are 2^1A and 3^1A.

The energy minimizes below 7.0 at 6.553 eV for the first excited (2^1A) state but with an oscillator strength of roughly 0.001. Again, this small oscillator strength does not provide promise for explaining the 200 nm peak from experiment. As a result, one-body properties are unlikely to correlate to the spectrum observed in ref 9, leaving dimer arrangements as the next logical avenue of exploration.

Dimer Analysis. The constrained scan of the carbonic acid dimer is depicted in Figure 2D with the transition properties shown in Figure 5. This scan defines θ as 180° minus the

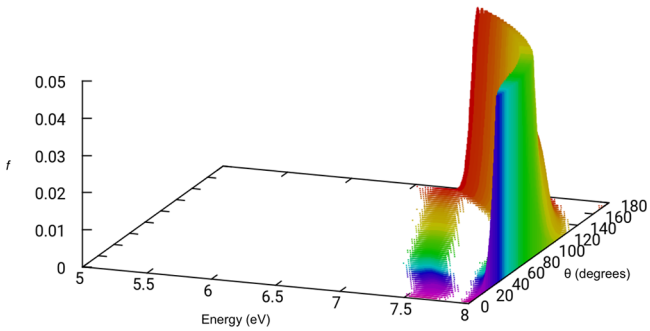

Figure 5. Scan (C_2) of the carbonic acid dimer, as shown in Figure 2D. The states reported (from left to right) are 2^1A and 1^1B.

dihedral angle defined from τ(O═C−C═O), where the C═O portions are the ketones in each of the two dimers. This scan moves the dimer structure from the optimized form at θ = 0° to a highly repulsive C_{2v} form at θ = 180° where the two hydrogen atoms are sterically interfering with one another as shown in the bottom-right of Figure 2D. While the excitations in Figure 5 decrease in energy, the higher oscillator strength 1^1B state transition does not dip into the sub-7.0 eV range until the molecule becomes sterically unfavored.

In order to avoid the steric issues present in the twist of the dimer, the external hydrogen atom torsional angles (Figure 6A,B) are scanned in Figures 7 and 8 in a manner similar to the

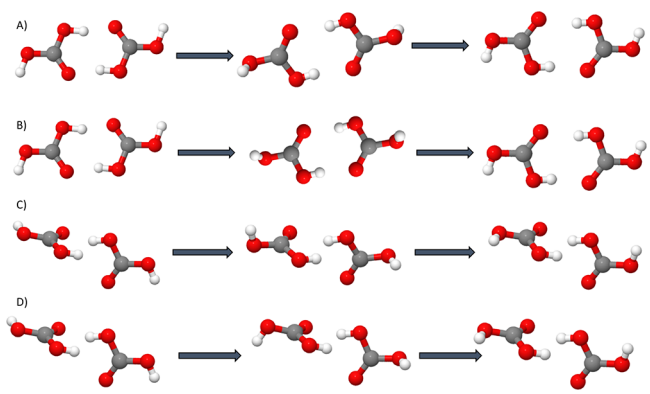

Figure 6. Visual depictions for the (A) conrotatory (C_2) scan of the external hydrogen atoms in the carbonic acid dimer, (B) disrotatory (C_1) scan of the external hydrogen atoms in the carbonic acid dimer, (C) disrotatory scan of the external hydrogen atoms in the 126° carbonic acid dimer, and (D) conrotatory scan of the external hydrogen atoms in the 126° carbonic acid dimer.

monomer in Figures 1 and 3. Only the external hydrogen atoms are displaced since the internal ones are needed to keep the dimer bound together. Separation of the dimer would likely simply recreate the monomer results in the previous section. The θ values for the hydrogen torsions are defined here from vectors pointing out-of-plane of each monomer such that, at θ = 90°, the hydrogens are in their in-plane equilibrium positions. These are then combined with the two monomers to define θ. Hence, at θ = 180°, the hydrogen atoms are perpendicular to the molecular planes of their respective monomers as shown in the middle of Figure 6A,B. The two

https://doi.org/10.1021/acs.jpca.2c07589
J. Phys. Chem. A XXXX, XXX, XXX−XXX

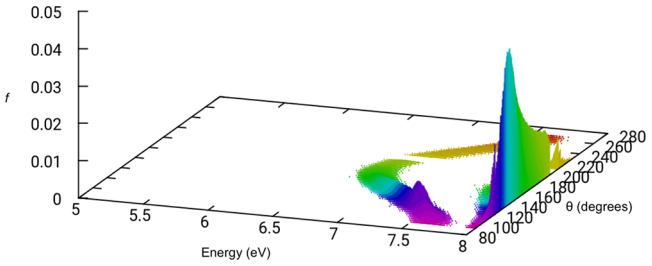

Figure 7. Conrotatory (C_2) scan of the external hydrogen atoms in the carbonic acid dimer (Figure 6A). The states reported (from left to right) are 2^1A and 1^1B.

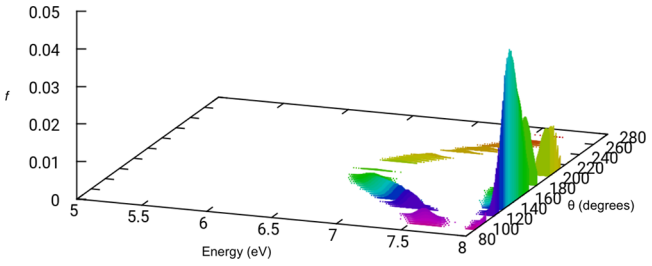

Figure 8. Disrotatory (C_1) scan of the external hydrogen atoms in the carbonic acid dimer (Figure 6B). The states reported (from left to right) are 2^1A and 3^1A.

scans are qualitatively the same with one another and exhibit similar properties as the corresponding monomers. They exhibit low oscillator strength first excited states that do not move much below 7.0 eV in contrast with the monomer states, but the higher-energy transitions are showing larger oscillator strengths. However, the energies of these states are still closer to 8.0 eV and are actually higher in energy than the second excited states in the monomer. Consequently, the displacements of the hydrogen atoms alone do not appear to be creating the conditions necessary to produce observable oscillator strengths for transitions at lower UV energies.

The next logical step then is to combine displacements of the dimer torsions themselves with scans of the hydrogen atom torsions. In starting from the displacements for the scan in Figure 5, these structures are then optimized with MP2/aug-cc-pVTZ with the torsion between the two dimers held constant. As mentioned above, the sterics on the hydrogen atoms as θ approaches 180° create disfavorable constructions, even if they promote lower-energy transitions. This leads to dissociation of the dimers for larger θ values. However, the largest θ to remain bound is for τ(O═C−C═O) = 126°, and this structure is 0.81 eV higher than the C_{2h} minimum at τ(O═C−C═O) = 0°. Hence, this torsion angle between the dimers themselves is utilized, followed by the previously employed disrotatory and conrotatory scans of the external hydrogen atom torsion angles.

These hydrogen scans of the τ(O═C−C═O) = 126° carbonic acid dimer are given in Figures 9 and 10. The disrotatory scan in Figure 9 produces transitions into the 2^1A state that approach 6.5 eV, but once more, the oscillator strengths are very low. This is even true for the higher-energy 3^1A state, which hovers around 7.5 eV. Hence, none of these states fall into the 5.5−7.0 eV range with large enough oscillator strengths needed to help explain the experimental spectrum observed in ref 9.

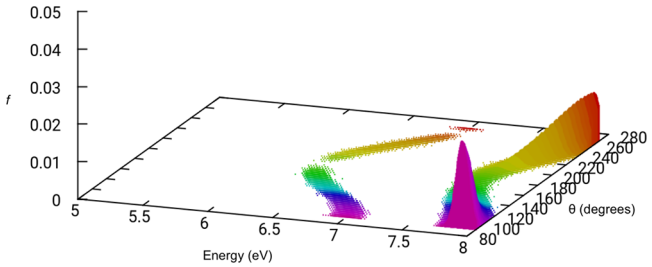

Figure 9. Disrotatory (C_1) scan of the external hydrogen atoms in the 126° displaced carbonic acid dimer (Figure 6C). The states reported (from left to right) are 2^1A and 3^1A.

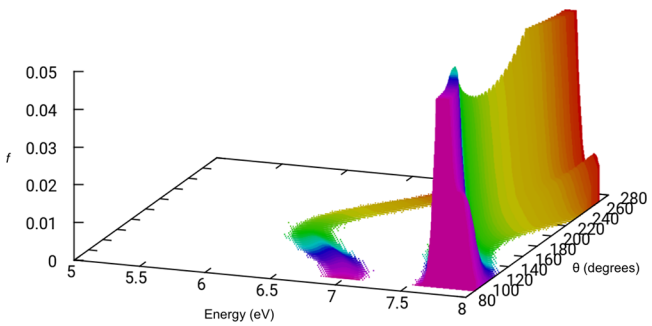

Figure 10. Conrotatory (C_1) scan of the external hydrogen atoms in the 126° displaced carbonic acid dimer (Figure 6D). The states reported (from left to right) are 2/3^1A and 4^1A.

In contrast, the conrotatory scan in Figure 10 defined in Figure 6D is somewhat more promising. The conrotatory maximum at θ = 180° is lower in energy than the structure at θ = 0°, since it lies 0.61 eV above the C_{2h} dimer minimum. The lowest-energy transition into the 2^1A excited state for this scan stretches down below 6.5 to 6.318 eV and has small but notable oscillator strengths on the order of 0.001 in this range as reported in Table S8 in the Supporting Information. However, the 3^1A state is nearly isoenergetic with the 2^1A state and has an oscillator strength of similar magnitude. As a result, these two states convolve together and produce an oscillator strength where the sum is notably greater than the parts.

This convolvement of the two lowest-energy transitions is teased out in Figure 11 where only one H atom is displaced out-of-plane for the τ(O═C−C═O) = 126° carbonic acid dimer. The 2 and 3 ^{1}A states are separated herein due to splittings in the two highest occupied molecular orbitals. The 3^1A state is largely unaffected by the scan since the previously

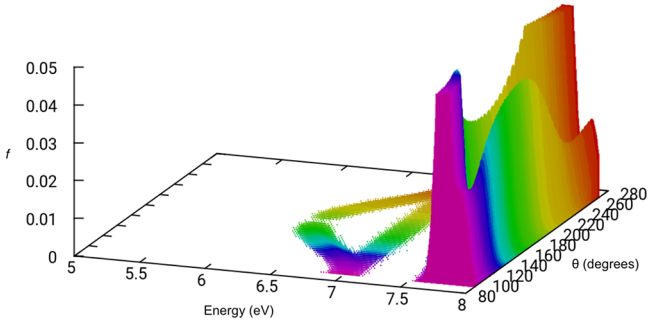

Figure 11. Scan (C_1) of a single external hydrogen atom in the 126° displaced carbonic acid dimer. The states reported (from left to right) are the 2−5^{1}A states.

https://doi.org/10.1021/acs.jpca.2c07589
J. Phys. Chem. A XXXX, XXX, XXX−XXX

paired orbitals in the con- and disrotatory scans are no longer so. In this scan, the accepting virtual orbitals split, since they are isolated on the monomer within the dimer where the hydrogen atom is not displaced. In any case, the separation of the states by the pseudosymmetry breaking reduces the peak height to just that of the individual parts. While this also drops the excitation energy to below 6.5 eV, the intensity of any observed peaks would be small. The higher-energy transitions have greater oscillator strengths, but they remain above 7.5 eV and could not contribute to the 200 nm feature.

A major hangup, however, is that, in order to access the 126° angle, an additional 100+ kcal/mol of energy (>4.4 eV; Figure S2) must be added to created this isomer, plus the energy needed to twist the hydrogen dihedrals. Such energy requirements would be on the order of the actual excitation energy we are attempting to model. While smaller dimer dihedrals would be more energetically favorable, the combination of Figures 6 and 7 could produce excitation energies in the desired range below 6.5 eV, but the oscillator strengths would likely still be small. Additionally, the ground states would require at least 20 kcal/mol (0.87 eV) to access these geometries. Furthermore, the odds of two nonminimum phenomena taking place simultaneously casts additional doubt on this pathway. As such, this leads to a rethinking of the distortions to be explored.

"Butterfly" Dihedral of the Monomer. In moving beyond motions of the hydrogen atoms or even the dimers themselves, the internal structure of carbonic acid is not as rigid as a central sp^2 carbon would imply. In fact, in a scan of the heavy atom, the τ(OCOO) dihedral ("butterfly") angle is actually relatively flat. While τ(OCOO) = 180° at the minimum geometry, when τ(OCOO) = 150°, the relative ground electronic state energy is only 11 kcal/mol (0.48 eV; Figure S3) above the minimum. By comparison, this same value is reached at 45° in the lower-energy C_2 scan of the hydrogen atom dihedral rotations of the monomer (the motion in Figure 1; energies in Figure S1) and at 30° for the dihedral angle between the two monomers in the dimer (Figure S2). Both of these latter two cases are considered floppy motions, in stark contrast to the dihedral motion of a typical ketone carbon. However, the present ketone carbon is also seemingly labile. This relatively floppy motion in carbonic acid almost certainly enables the proclivity of carbonic acid to return to carbon dioxide and water since the smaller τ(OCOO) values allow the OH groups to come closer together increasing the likelihood of hydrogen transfer producing water. Even so, once τ(OCOO) crosses 135° on approach to 90° (Figure S3) and roughly 30 kcal/mol (1.3 eV), the relative energy of the ground state increases rapidly, implying that these distortions are limited to a range of roughly 45° or less about the equilibrium geometry's planarity.

The scan of the excited states for this "butterfly" dihedral angle of the carbonic acid monomer is shown in Figure 12. The scan is stopped at 141° due to energetic considerations. However, beyond τ(OCOO) = 156°, the $1^1A''$ state drops below 6.5 eV with oscillator strengths on the order of 1×10^{-2}, the exact range needed to inform the spectrum in ref 9. The distortion to the geometry is enough to bring this $n \rightarrow \pi^*$ excitation energy down and the oscillator strength up. As shown in Table S10, the value of the oscillator strength drops by an order of magnitude over the first 30° of the τ(OCOO) scan, and the excitation energy drops by more than 1.0 eV. While the excitation energy for this state and that of most

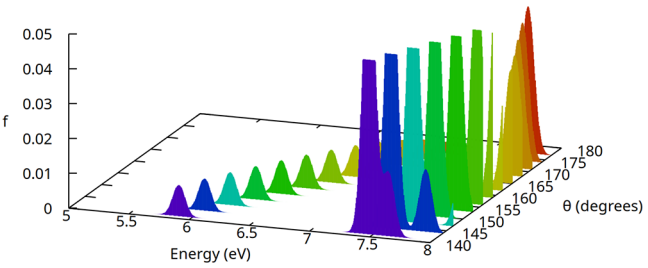

Figure 12. Scan (C_s) of the τ(OCOO) dihedral (butterfly) angle of the carbonic acid monomer. The states reported (from left to right) are the $1^1A''$, $2^1A'$, and $2^1A''$ states.

others continues to drop values even below 5 eV, the higher energy of the ground state likely minimizes these structures' contribution. Additionally, the oscillator strength remains at roughly 1×10^{-2} all the way to τ(OCOO) = 114° when it begins to reduce. In any case, this low-energy ground-state energy for this surprisingly floppy motion has the excitation energy and oscillator strength that would line up with the secondary peak shown in ref 9.

CONCLUSIONS

The relatively low potential energy for the distortion of the internal τ(OCOO) dihedral angle also produces structures with $n \rightarrow \pi^*$ excitation energies below 6.5 eV with notable oscillator strengths. Additionally, these floppy, nonminimum geometries will be widely varied in terms of their displacements causing a spread of excitation energies. This behavior would cause a broad feature like that observed in ref 9. The optimization of the amorphous clusters in ref 12 may actually inhibit access to these nonminima structures, reducing their ability to contribute to the spectrum. While such optimizations are likely acceptable for most applications, the nature of the 20 K annealing in ref 9 and the floppy nature of carbonic acid itself appear to provide a more complicated picture that may only be explained by the inclusion of nonminima arrangements of the carbonic acid molecules in clusters.

This present work shows that, for nonminimum, symmetry-broken carbonic acid, twisting the hydrogen atom torsional angles in the monomers strongly reduces the excitation energy down to nearly 6.0 eV right where the 200 nm feature has been previously observed.[9] However, the oscillator strength remained small. The same motion in the dimers actually has a less red-shifting effect. Scanning over the dihedral space between the monomers in the dimer reduces the excitation energy but leads to unstable structures. Taking the intermonomer τ(O=C−C=O) = 126° angle and then also scanning over the external hydrogen atom dihedrals in the dimer brings the excitation energy back to less than 6.5 eV. Additionally, the conrotatory scan then allows for two electronic states to combine at these energies and, therefore, increase the intensity of the convolved peak to greater than the sum of the parts. However, the energy required to produce such structures is nearly the same as the excitation energy itself. The butterfly dihedral of the heavy atoms in the monomer, however, is a relatively low-energy motion below 180° down to 141° where the excitation energies and oscillator strength magnitudes are the closest match for the ∼200 nm peak observed by Ioppolo and co-workers.[9]

https://doi.org/10.1021/acs.jpca.2c07589
J. Phys. Chem. A XXXX, XXX, XXX−XXX

■ ASSOCIATED CONTENT

Supporting Information

The Supporting Information is available free of charge at https://pubs.acs.org/doi/10.1021/acs.jpca.2c07589.

The electronically excited state data computed in this work and utilized to produce the figures as well as the scans of the ground relative energies for the hydrogen dihedral of the monomer, the dihedral, and the butterfly dihedral (PDF)

■ AUTHOR INFORMATION

Corresponding Author

Ryan C. Fortenberry − *Department of Chemistry & Biochemistry, University of Mississippi, University, Mississippi 38677-1848, United States;* orcid.org/0000-0003-4716-8225; Email: r410@olemiss.edu

Authors

Olivia G. Haney − *Department of Chemistry & Biochemistry, Belhaven University, Jackson, Mississippi 39212, United States*

Brent R. Westbrook − *Department of Chemistry & Biochemistry, University of Mississippi, University, Mississippi 38677-1848, United States;* orcid.org/0000-0002-6878-0192

Taylor J. Santaloci − *Department of Chemistry & Biochemistry, University of Mississippi, University, Mississippi 38677-1848, United States*

Complete contact information is available at: https://pubs.acs.org/10.1021/acs.jpca.2c07589

Notes

The authors declare no competing financial interest.

■ ACKNOWLEDGMENTS

This work is supported by NSF Grant Nos. OIA-1757220 & CHE-1757888, NASA Grant No. NNX17AH15G, the Mississippi Space Grant Consortium, and the University of Mississippi's College of Liberal Arts. The computational resources for this work are provided by the Mississippi Center for Supercomputing Research. The authors would also like to acknowledge Profs. D. B. Magers and S. Smith of Belhaven University for their support of this work.

■ REFERENCES

(1) Zheng, W.; Kaiser, R. I. On the Formation of Carbonic Acid (H_2CO_3) in Solar System Ices. *Chem. Phys. Lett.* **2007**, *450*, 55−60.

(2) Sandford, S. A.; Nuevo, M.; Bera, P. P.; Lee, T. J. Prebiotic Astrochemistry and the Formation of Molecules of Astrobiological Interest in Interstellar Clouds and Protostellar Disks. *Chem. Rev.* **2020**, *120*, 4616−4659.

(3) Reisenauer, H. P.; Wagner, J. P.; Schreiner, P. R. Gas-Phase Preparation of Carbonic Acid and Its Monomethyl Ester. *Angew. Chem. Int. Ed.* **2014**, *53*, 11766−11771.

(4) Köck, E.; Bernard, J.; Podewitz, M.; Dinu, D. F.; Huber, R. G.; Liedl, K. R.; Grothe, H.; Bertel, E.; Schlögl, R.; Loerting, T. Alpha-Carbonic Acid Revisited: Carbonic Acid Monomethyl Ester as a Solid and Its Conformational Isomerism in the Gas Phase. *Chem.-Eur. J.* **2020**, *26*, 285−305.

(5) Zhu, C.; Kleimeier, N. F.; Turner, A. M.; Singh, S. K.; Fortenberry, R. C.; Kaiser, R. I. Synthesis of Methanediol [$CH_2(OH)_2$]: The Simplest Geminal Diol. *Proc. Natl. Acad. Sci. U.S.A.* **2022**, *119*, No. e2111938119.

(6) Jian, H.-Y.; Yang, C.-T.; Chu, L.-K. Gaseous Infrared Spectra of the Simplest Geminal Diol $CH_2(OH)_2$ and the Isotopic Analogues in the Hydration of Formaldehyde. *Phys. Chem. Chem. Phys.* **2021**, *23*, 14699−14705.

(7) Davis, M. C.; Garrett, N. R.; Fortenberry, R. C. Confirmation of Gaseous Methanediol from State-of-the-Art Theoretical Rovibrational Characterization. *Phys. Chem. Chem. Phys.* **2022**, *24*, 18552−18558.

(8) Jones, B. M.; Kaiser, R. I.; Strazzulla, G. Carbonic Acid as a Reserve of Carbon Dioxide on Icy Moons: The Formation of Carbon Dioxide (CO_2) in a Polar Environment. *Astrophys. J.* **2014**, *788*, 170.

(9) Ioppolo, S.; Kanuchová, Z.; James, R. L.; Dawes, A.; Ryabov, A.; Dezalay, J.; Jones, N. C.; Hoffmann, S. V.; Mason, N. J.; Strazzulla, G. Vacuum Ultraviolet Photoabsorption Spectroscopy of Space-Related Ices: Formation and Destruction of Solid Carbonic Acid upon 1 keV Electron Irradiation. *Astron. Astrophys.* **2021**, *646*, A172.

(10) Wallace, A. M.; Fortenberry, R. C. Linear and Helical Carbonic Acid Clusters. *J. Phys. Chem. A* **2021**, *125*, 4589−4597.

(11) Pavithraa, S.; Lo, J.-I.; Cheng, B.-M.; Sekhar, B. N. R.; Mason, N. J.; Sivaraman, B. Identification of a Unique VUV Photoabsorption Band of Carbonic Acid for its Identification in Radiation and Thermally Processed Water-Carbon Dioxide Ices. *Spectrochim. Acta, Part A* **2019**, *215*, 130−132.

(12) Wallace, A. M.; Fortenberry, R. C. Theoretical Characterization of Carbonic Acid Clusters in the UV. *J. Phys. Chem. A* **2022**, *126*, 3739−3744.

(13) M Wallace, A.; C Fortenberry, R. Computational UV Spectra for Amorphous Solids of Small Molecules. *Phys. Chem. Chem. Phys.* **2021**, *23*, 24413−24420.

(14) Møller, C.; Plesset, M. S. Note on an Approximation Treatment for Many-Electron Systems. *Phys. Rev.* **1934**, *46*, 618−622.

(15) Dunning, T. H. Gaussian Basis Sets for Use in Correlated Molecular Calculations. I. The Atoms Boron through Neon and Hydrogen. *J. Chem. Phys.* **1989**, *90*, 1007−1023.

(16) Kendall, R. A.; Dunning, T. H.; Harrison, R. J. Electron Affinities of the First-Row Atoms Revisited. Systematic Basis Sets and Wave Functions. *J. Chem. Phys.* **1992**, *96*, 6796−6806.

(17) Scheiner, A. C.; Scuseria, G. E.; Rice, J. E.; Lee, T. J.; Schaefer, H. F., III Analytic Evaluation of Energy Gradients for the Single and Double Excitation Coupled Cluster (CCSD) Wave Function: Theory and Application. *J. Chem. Phys.* **1987**, *87*, 5361−5373.

(18) Stanton, J. F.; Bartlett, R. J. The Equation of Motion Coupled-Cluster Method - A Systematic Biorthogonal Approach to Molecular Excitation Energies, Transition-Probabilities, and Excited-State Properties. *J. Chem. Phys.* **1993**, *98*, 7029−7039.

(19) Crawford, T. D.; Schaefer, H. F., III. In *Reviews in Computational Chemistry;* Lipkowitz, K. B., Boyd, D. B., Eds.; Wiley: New York, 2000; Vol. *14*; pp 33−136.

(20) Nguyen, Q. L.; Peters, W. K.; Fortenberry, R. C. Highly-Excited State Properties of Cumulenone Chlorides in the Vacuum-Ultraviolet. *Phys. Chem. Chem. Phys.* **2020**, *22*, 11838−11849.

(21) Werner, H.-J.; Knowles, P. J.; Knizia, G.; Manby, F. R.; Schütz, M. Molpro: A General-Purpose Quantum Chemistry Program Package. *WIREs Comput. Mol. Sci.* **2012**, *2*, 242−253.

(22) Werner, H.-J.; Knowles, P. J.; Knizia, G.; Manby, F. R.; Schütz, M.; Celani, P.; Györffy, W.; Kats, D.; Korona, T.; Lindh, R.; et al. 2020; see http://www.molpro.net; Accessed: 2022-05-05.